DOI: 10.1002/cbic.200700433

# Pyrazolyl–Diamine Ligands That Bear Anthracenyl Moieties and Their Rhenium(I) Tricarbonyl Complexes: Synthesis, Characterisation and DNA-Binding Properties

Rute F. Vitor,[a] Isabel Correia,[b] Margarida Videira,[a] Fernanda Marques,[a] António Paulo,[a] João Costa Pessoa,[b] Giampietro Viola,[c] Gabriel G. Martins,[d] and Isabel Santos*[a]

*Two novel families of pyrazolyl–diamine ligands that bear an anthracen-9-yl group as a DNA-binding fragment, pz*$(CH_2)_2$NH$(CH_2)_2$NHCH$_2$-9-anthryl (pz* = pz (**L$^1$**), 3,5-Me$_2$pz (**L$^2$**)) and pz*$(CH_2)_2$NH$(CH_2)_2$NH$_2$ (pz* = 4-(9-anthrylmethyl)pz (**L$^3$**), 3,5-Me$_2$-4-(9-anthrylmethyl)pz (**L$^4$**)), have been prepared and fully characterised. In the case of **L$^2$**–**L$^4$**, the evaluation of their coordination capability towards the fac-[Re(CO)$_3$]$^+$ core led to the synthesis of the organometallic complexes fac-[Re(CO)$_3${3,5-Me$_2$pz$(CH_2)_2$NH$(CH_2)_2$NHCH$_2$-9-anthryl}]Br (**7**) and fac-[Re(CO)$_3${4-(9-anthrylmethyl)pz*$(CH_2)_2$NH$(CH_2)_2$NH$_2$}]Br (pz* = pz (**8**), 3,5-Me$_2$pz (**9**)). The interaction of the novel pyrazole–diamine ligands and the rhenium(I) complexes with calf thymus (CT) DNA has been investigated with a variety of spectroscopic techniques (UV-visible, fluorescence, circular dichroism (CD) and linear dichroism (LD)). All of the evaluated compounds have a moderate affinity to CT DNA ($3.46\times10^3 < K_b < 1.95\times10^4$), but the binding mode depends on the position of the chromophore in the framework of the pyrazolyl–diamine ligands. LD measurements have shown that **L$^1$** and **L$^2$** act as DNA intercalators, but complex **7** intercalates only partially. By contrast, the compounds with the anthracenyl group at the 4-position of the azolyl ring (**L$^3$**, **L$^4$** and **9**) do not intercalate, and behave more like DNA groove binders. Fluorescence microscopy studies have demonstrated that complexes **7** and **9** can target the nucleus of murine B16-F1 melanoma cells, and appear to be promising platforms for the further design of radiopharmaceuticals for targeted radiotherapy.*

## Introduction

The targeted therapy of cancer with radiometals is gaining relevance as a therapeutic alternative to conventional methodologies, such as surgery, external radiotherapy and chemotherapy.[1,2] Interestingly, several gamma-emitting radiometals that are routinely applied in diagnostic nuclear medicine, such as $^{99m}$Tc or $^{111}$In, are also Auger electron-emitters and therefore their complexes could also have potential in targeted tumour therapy. Although some promising results have been already reported for $^{111}$In complexes that contain bioactive peptides,[3,4] the therapeutic potential of Auger emitter radiometals has not yet been fully demonstrated in the clinical arena.

Due to the short range of Auger electrons, there is a need for preferential accumulation of the complexes into the nucleus of neoplastic cells in order to elicit significant DNA damage, and therefore a therapeutic effect. The achievement of this goal lies in the design of multifunctional complexes that include a DNA-binding moiety, a carrier to transport the complex into the nucleus, and/or a tumour-seeking vector.[4–6] The presence of the later should provide a specific recognition of the neoplastic cells and promote the internalisation of the complexes, while the DNA-binding moiety is expected to augment the stacking into DNA, and consequently to enhance the radiotoxicity of the Auger emitter.

Technetium-99m is the most widely used radionuclide in diagnostic nuclear medicine; this is because it has ideal nuclear properties and is inexpensive and widely available. Encouraging in vitro results have been reported that highlighted the relevance of this radiometal for the development of therapeutic radiopharmaceuticals.[5–7] Alberto et al. have shown that a $^{99m}$Tc$^{I}$–tricarbonyl complex that contains a pyrene intercalator and a nuclear localisation signal (NLS) peptide can target the nucleus of B16-F1 mouse melanoma cells, and shows a much stronger radiotoxic effect than $^{99m}TcO_4^-$, which is unable to penetrate the nucleus.[6] Most importantly, the same research group proved more recently that the presence of the NLS sequence is not strictly necessary for the targeting of the nucleus with tricarbonyl $^{99m}$Tc$^{I}$ or Re$^{I}$ complexes.[7]

[a] *R. F. Vitor, M. Videira, Dr. F. Marques, Dr. A. Paulo, Dr. I. Santos*
*Departamento de Química, ITN*
*Estrada Nacional 10, 2686-953 Sacavém Codex (Portugal)*
*Fax: (+351) 21-994-14-55*
*E-mail: isantos@itn.pt*

[b] *Dr. I. Correia, Prof. J. Costa Pessoa*
*Centro de Química Estrutural*
*Instituto Superior Técnico, TU Lisbon*
*Av. Rovisco Pais 1, 1049-001 Lisbon (Portugal)*

[c] *Dr. G. Viola*
*Department of Pharmaceutical Sciences*
*University of Padova*
*via Marzolo 5, 35131 Padova (Italy)*

[d] *Dr. G. G. Martins*
*Instituto Gulbenkian da Ciência*
*Apartado 14, 2781-901 Oeiras (Portugal)*

*Supporting information for this article is available on the WWW under http://www.chembiochem.org or from the author:UV-visible and fluorescence spectroscopy titrations of **L$^1$** and **L$^3$** with CT DNA; Scatchard plot of the UV-visible spectroscopy data for **L$^1$**–**L$^4$**, **7** and **9**; McGhee–von Hippel binding isotherms for the fluorescence data of **L$^1$** and **L$^2$**.*

  

Within our interest on Re and Tc complexes for biomedical applications, we have introduced bifunctional chelators of the pyrazole–diamine type, which act as powerful tridentate chelators towards the *fac*-$[M(CO)_3]^+$ (M = Re, $^{99m}$Tc) moiety, and form tricarbonyl complexes with excellent in vitro and in vivo stability.[8,9] These chelators are easily modified with biologically active molecules, and have been applied already in the labelling of small tumour-seeking peptides, which have delivered encouraging results in terms of their biological behaviour.[10–12] Due to their versatile nature, these pyrazolyl–diamine chelators allow also the introduction of DNA-binding groups at different positions of the ligand framework, namely at the 4-position of the pyrazolyl ring or at the terminal primary amine, while the option of using the central amine for coupling a tumour-seeking vector is still available (Scheme 1). By taking these favourable features into account, we have anticipated that these systems could be useful tools for the design of multifunctional complexes, with the goal of developing $^{99m}$Tc radiopharmaceuticals for targeted radiotherapy. As a first step in this design process, we explored the possibility of introducing 9-anthrylmethyl fragments at the 4-position of the azole ring and at the terminal amine of pyrazolyl–diamine ligands, then we studied the coordination capability of the resulting chelators towards the *fac*-$[Re(CO)_3]^+$ moiety with the aim of introducing novel complexes that are able to enter the nucleus and interact with DNA.

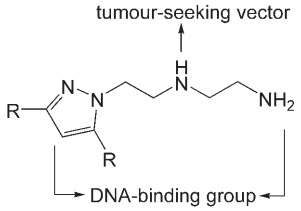


**Scheme 1.** Schematic representation of different possibilities for the functionalisation of pyrazoyl–diamine chelators with a tumour-seeking vector and/or a DNA-binding group.

Re and Tc complexes are usually isostructural, and therefore, the Re complexes are considered to be adequate surrogates for the $^{99m}$Tc congeners, which are prepared only in $10^{-9}$–$10^{-7}$ M concentrations, and can not be characterised by the common analytical techniques of inorganic and organometallic chemistry. Moreover, with the compounds proposed herein, we also intended to profit from the fluorescent properties of the anthracenyl moiety and to use the Re complexes to evaluate in vitro the cellular uptake of the compounds by fluorescence microscopy.

In this work, we introduce a series of novel pyrazolyl-containing ligands that bear an anthracenyl derivative as a DNA-binding fragment, pz*$(CH_2)_2NH(CH_2)_2NHCH_2$-9-anthryl (pz* = pz, **L$^1$**; 3,5-$Me_2$pz, **L$^2$**) and pz*$(CH_2)_2NH(CH_2)_2NH_2$ (pz* = 4-(9-anthrylmethyl)pz, **L$^3$**; 3,5-$Me_2$-4-(9-anthrylmethyl)pz, **L$^4$**), and report on the synthesis and characterisation of the Re$^I$–tricarbonyl complexes that are anchored onto **L$^2$**–**L$^4$** (**7**–**9**). The interaction of DNA with the novel pyrazole–diamine ligands (**L$^1$**–**L$^4$**) and with the Re$^I$ complexes **7** and **9** has been evaluated by using different spectroscopic techniques (UV/vis, circular dichroism (CD), linear dichroism (LD) and fluorescence) and is also reported. We also present fluorescence microscopy studies on the uptake of selected ligands and complexes in B16-F1 mouse melanoma cells. This work also addresses how the position that is used to attach the anthracenyl fragment to the chelator framework and/or the introduction of the organometallic *fac*-$[Re(CO)_3]^+$ moiety will influence the interaction with DNA and/or the ability of the compounds to enter the cells and to target the nucleus.

## Results and Discussion

By choosing the anthracenyl fragment as a DNA binder and by exploring its conjugation to different points of the pyrazolyl–diamine framework, we have taken into consideration the well-known ability of the planar and polycyclic structure of anthracene to intercalate between neighbouring base pairs, the versatility of functionalisation of the pyrazolyl–diamine chelators, and their potential to stabilise the *fac*-$[M(CO)_3]^+$ core (M = Re, $^{99m}$Tc).[10–12] Moreover, anthracenyl chromophores have a moderate molar absorptivity in the near-UV region and good fluorescence quantum yields; this allows the study of the binding of the ligands and the respective Re complexes with DNA by spectroscopic techniques, as well as the evaluation of their cellular uptake by fluorescence microscopy.[13]

### Synthesis of anthracenyl-containing chelators and their Re complexes

For the incorporation of the anthracenyl fragment at the terminal amine of the pyrazolyl–diamine chelators, we have explored the reductive amination of the commercially available 9-anthracenealdehyde; this is a synthetic approach that has been already used successfully by other authors to prepare *N*-anthracenyl-9-ylmethyl conjugates of biogenic polyamines, like spermidine.[14,15] As depicted in Scheme 2, the reaction of 9-anthracenealdehyde with the compounds [pz*$(CH_2)_2NH(CH_2)_2NH_2$] (pz* = pz, 3,5-$Me_2$pz), which have been previously described by our group,[8,10] afforded the corresponding imine derivatives. The in situ reduction of these imines with sodium borohydride yielded the final ligands pz*NN-Ant (pz* = pz, **L$^1$**; 3,5-$Me_2$pz, **L$^2$**). These compounds were isolated in moderate to high yield after purification by silica gel column chromatography. Throughout the paper we will adopt the abbreviation pz*NN-Ant for the ligands that have the anthracenyl moiety at the terminal amine and the abbreviation Ant-pz*NN for those with the same moiety at the 4-position of the pyrazolyl ring.

The introduction of the anthracenyl-9-yl methyl group at the 4-position of the azolyl ring has been demanding, and required the preparation of the dicarbonyl compounds [2-(9-anthrylmethyl)propane-1,3-dialdehyde] (**1**) and [2-(9-anthrylmethyl)-pentane-2,4-dione] (**2**), as shown in Scheme 3. The 1,3-dialdehyde **1** was prepared by a Swern oxidation of the corresponding diol with DMSO/$SO_3$·pyridine, while the synthesis of the

  

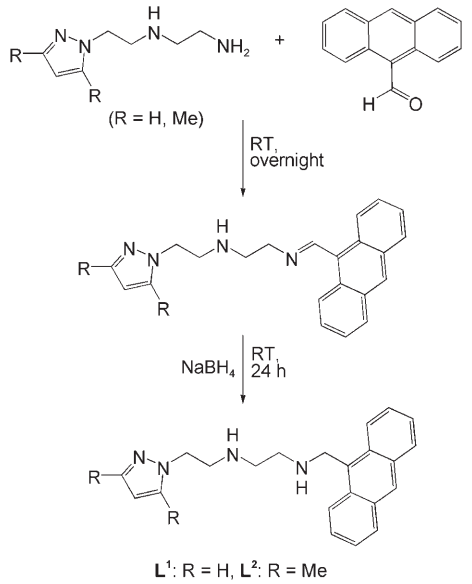


**Scheme 2.** Synthesis of the pyrazole–diamine chelators that bear a terminal anthracene chromophore. o.n. = overnight.

1,3-diketone **2** was accomplished by alkylation of acetylacetone with 9-bromomethylanthracene. Compounds **1** and **2** are yellow oils, and were obtained in the enol and keto forms, respectively. The cyclisation of **1** and **2** with 2-hydroxyethylhydrazine gave the pyrazole derivatives Ant-pz*$(CH_2)_2$OH (pz* = pz, **3**; 3,5-$Me_2$pz, **4**) which were brominated with $PBr_3$ to afford the compounds Ant-pz*$(CH_2)_2$Br (pz* = pz, **5**; 3,5-$Me_2$pz, **6**). Treatment of **5** and **6** with a 20-fold molar excess of ethylenediamine in refluxing methanol led to the formation of the final ligands, Ant-pz*NN (pz* = pz, $L^3$; 3,5-$Me_2$pz, $L^4$), which have been isolated as yellow oils in moderate yields (39–50%) after chromatographic purification.

The novel anthracenyl-containing pyrazole–diamine ligands $L^1$–$L^4$ are air and water-stable compounds. They are soluble in common organic solvents, but only sparingly soluble in aqueous medium. The characterisation of $L^1$–$L^4$ has been performed by $^1$H and $^{13}$C NMR spectroscopy. FT-ICR mass spectrometry confirmed the authenticity of these ligands because prominent $[M+H]^+$ peaks were obtained at *m/z* 345.2 ($L^1$ and $L^3$) and at *m/z* 373.2 ($L^2$ and $L^4$).

The evaluation of the coordination capability of the anthracenyl-containing ligands towards the *fac*-$[Re(CO)_3]^+$ core comprised the study of their reaction with the starting material $[Re(CO)_5Br]$. In refluxing methanol, the reaction with $L^2$–$L^4$ led to the formation of well-defined species that were formulated as *fac*-$[Re(CO)_3\{3,5\text{-}Me_2pzNN\text{-}Ant\}]Br$ (**7**) and *fac*-$[Re(CO)_3\{Antpz^*NN\}]Br$ (pz* = pz, **8**; 3,5-$Me_2$pz, **9**) (Scheme 4). Compounds **7**–**9** were the unique complexes that were formed; this was confirmed by $^1$H NMR analysis of the crude after removal of the solvent. Nevertheless, **7** and **8** were isolated in poor to moderate yields due to the need for recrystallisation or washing to remove small amounts of the unreacted ligands.

Complexes **7**–**9** are yellow microcrystalline solids, which are stable towards hydrolysis or aerial oxidation. They were characterised by IR, $^1$H and $^{13}$C NMR spectroscopies, as well as by ESI-MS spectrometry. As for the corresponding ligands, we could not obtain satisfactory elemental analysis for **7**–**9**, even though the $^1$H and $^{13}$C NMR spectra showed a high bulk purity for these compounds. The ESI-MS analysis showed the expected

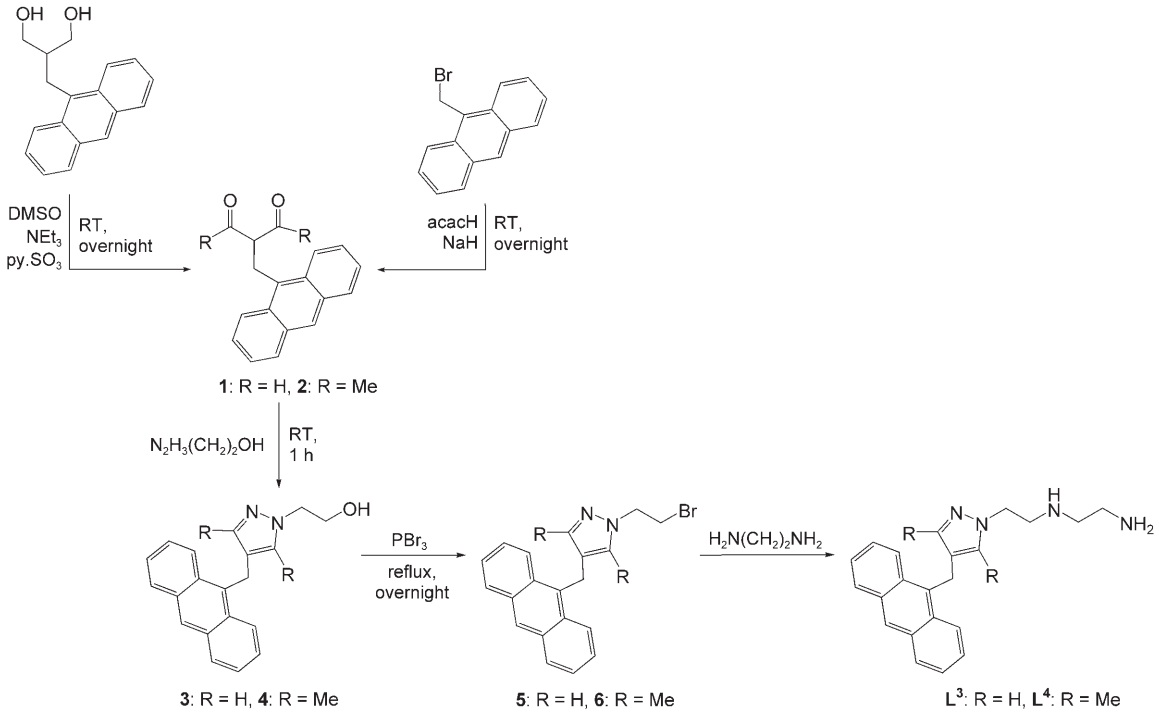


**Scheme 3.** Synthesis of the pyrazole–diamine chelators that bear an anthracene chromophore at the 4-position of the azolyl ring.

  

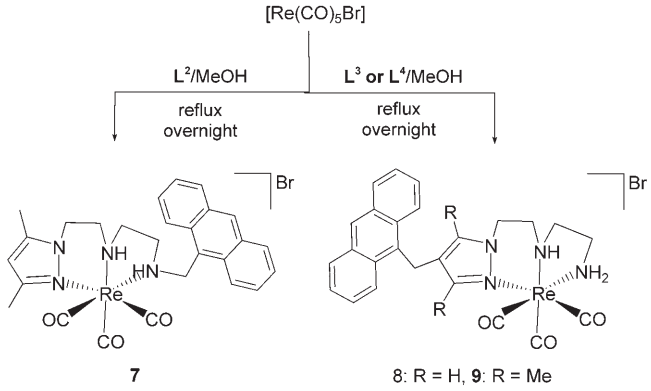


**Scheme 4.** Synthesis of the $Re^{I}$–tricarbonyl complexes.

molecular ions at *m/z* 643.0 (**7** and **9**) and 614.9 (**8**), which confirms the proposed formulation.

The IR spectra of **7**–**9** showed the presence of two intense $\nu$(C≡O) bands in the region 2026–1896 $cm^{-1}$, which is typical of complexes with the *fac*-$[Re(CO)_3]^+$ moiety. The frequencies of these bands are almost coincident with the values that we have previously found for other $Re^{I}$–tricarbonyl complexes that are anchored by the same pyrazolyl–diamine framework.[8–10] The comparison of the $^1$H NMR spectra of *fac*-$[Re(CO)_3${Ant-pz*NN}]Br (pz* = pz, **8**; 3,5-$Me_2$pz, **9**) with the previously described *fac*-$[Re(CO)_3${pz*$(CH_2)_2NH(CH_2)_2NH_2$}]Br (pz* = pz, 3,5-$Me_2$pz) showed that they are almost superimposable, except for the presence of the resonances that are due to the 9-anthrylmethyl substituent.[8–10] The similarities between the spectra allowed us to conclude that in **8** and **9** the anthracenyl-containing ligands are coordinated in a tridentate fashion through the pyrazole and the amine nitrogen atoms; we have previously confirmed this particular coordination mode by X-ray crystallography for other complexes of this type.[8]

For the complex that contains a terminal 9-anthrylmethyl group, *fac*-$[Re(CO)_3${3,5-$Me_2$pzNNAnt}] (**7**), the chemical shifts and splitting of the diasterotopic methylenic protons from the pyrazolyl–diamine backbone are very similar to those of **8** and **9**. For **7**, only two broad singlets for the NH protons appear at 7.18 and 4.36 ppm, while for **8** and **9** three NH resonances could be identified (**8**: 6.93, 5.26 and 3.41 ppm; **9**: 6.90, 5.38 and 3.82 ppm). In the spectrum of **7**, the two multiplets that appear at 5.37 and 5.55 ppm were assigned to the $CH_2$ protons that link the anthracene moiety and the terminal amine. This splitting indicates diastereotopic character for those protons, and it confirms the coordination of the terminal amine to the $Re^{I}$ centre, in spite of the presence of the bulkier 9-anthrylmethyl substituent.

For *fac*-$[Re(CO)_3${3,5-$Me_2$pzNN-Ant}]Br (**7**), the formation of two diastereomeric pairs of enantiomers was possible due to the presence of two chiral centres upon the coordination of $\mathbf{L^2}$. However, the $^1$H and $^{13}$C NMR data that were obtained for **7** clearly demonstrated that only one pair of enantiomers was formed. This result has also been confirmed by HPLC analysis of the compound (results not shown). Unexpectedly, the congener ligand $\mathbf{L^1}$, which lacks the methyl substituents at the 3- and 5-positions of the azolyl ring showed a quite different behaviour. The reactions of pzNN-Ant, $\mathbf{L^1}$ with $[Re(CO)_5Br]$ or $[NEt_4][Re(CO)_3Br_3]$ always afforded a mixture of complexes, regardless of which solvent (methanol or acetonitrile), temperature and reaction time was used. $^1$H NMR spectroscopy analysis of the crude of these reactions always indicated the formation of two major complexes because two dominant triplets for the H(4) protons of the pyrazolyl ring were observed. In $CD_3OD$, these protons resonate at 6.48 and 6.75 ppm; they are upfield shifted compared to the corresponding protons in the free ligand. Moreover, the spectra displayed a set of multiplets for the methylenic protons, the chemical shifts and splitting of which were very similar to those that were obtained for complex **7**. Taken together, these data suggest the presence of the two possible diastereomeric pairs of enantiomers for complex *fac*-$[Re(CO)_3${pzNN-Ant}]Br. We were unable to separate the two pairs of enantiomers, and other small contaminants were present. For this reason, the $Re^{I}$–tricarbonyl complex with $\mathbf{L^1}$ is not reported or evaluated here. Alberto et al. have already found a similar behaviour for related $Re^{I}$ complexes that are anchored by aliphatic triamine ligands that are terminally functionalised with pyrene or anthraquinone moieties.[5] These authors reported that two diastereomeric pairs of complexes were obtained for the pyrene-containing triamines, but a preferential formation of one pair of enantiomers was observed for the anthraquinone derivative. These differences might reflect the presence of planar aromatic structures such as pyrene or anthraquinone that have different steric constraints. This is not the case for the ligands pz*NN-Ant (pz* = pz, $\mathbf{L^1}$), 3,5-$Me_2$pz ($\mathbf{L^2}$), which contain a common anthracenyl fragment. The reasons behind their different behaviour are not yet clear.

## DNA-binding studies

UV-visible, fluorescence, CD and LD spectroscopies were used to study the binding of the ligands ($\mathbf{L^1}$–$\mathbf{L^4}$) and the $Re^{I}$–tricarbonyl complexes **7** and **9** to CT DNA. The low solubility in aqueous medium of **8**, even in the presence of dimethylsulfoxide, precluded the possibility of evaluating the interaction of this compound with DNA.

## UV-visible spectroscopy studies

For the different compounds under analysis, the UV/vis absorption studies comprised the monitoring of the changes on the bands due to the antracenyl chromophore upon addition of increasing amounts of CT DNA.

The UV-visible titrations of the molecules that contain the anthracenyl moiety at the terminal amine ($\mathbf{L^1}$, $\mathbf{L^2}$ and complex **7**) have shown that the absorption peaks of the anthracenyl chromophores are red shifted upon binding to DNA, as indicated in Table 1, and exemplified in Figure 1 for $\mathbf{L^2}$ and complex **7**. The ligands $\mathbf{L^1}$ and $\mathbf{L^2}$ display red shifts of 6 and 5 nm, respectively, which are more pronounced than the 2 nm shift that was obtained for the $Re^{I}$ complex **7**.

Isosbestic points were also evident in the spectra of $\mathbf{L^1}$, $\mathbf{L^2}$ and complex **7**; they appeared at 393 nm for $\mathbf{L^1}$ and $\mathbf{L^2}$ and at

  

**Table 1.** Hypochromism, red shifts and intrinsic binding constants for the ligands of types pz*NNAnt and Ant-pz*NN, and for their Re complexes.

| Compound | Hypochromism [%] | Red shift [nm] | $K_b$ [$M^{-1}$] |
|---|---|---|---|
| pzNN-Ant (**L**[1]) | 58 (366 nm) | 6 | $(4.25\pm0.08)\times10^3$ |
| 3,5-$Me_2$pzNN-Ant (**L**[2]) | 66 (366 nm) | 5 | $(3.46\pm0.04)\times10^3$ |
| Ant-pzNN (**L**[3]) | 34 (368 nm) | $<0.5$ | $(6.77\pm0.04)\times10^3$ |
| Ant-3,5-$Me_2$pzNN (**L**[4]) | 38 (367 nm) | $<0.5$ | $(1.06\pm0.01)\times10^4$ |
| *fac*-[Re(CO)$_3${3,5-$Me_2$pzNN-Ant}] (**7**) | 45 (372 nm) | 2 | $(2.20\pm0.01)\times10^3$ |
| *fac*-[Re(CO)$_3${Ant-3,5-$Me_2$pzNN}] (**9**) | 57 (367 nm) | $<0.5$ | $(1.95\pm0.01)\times10^4$ |

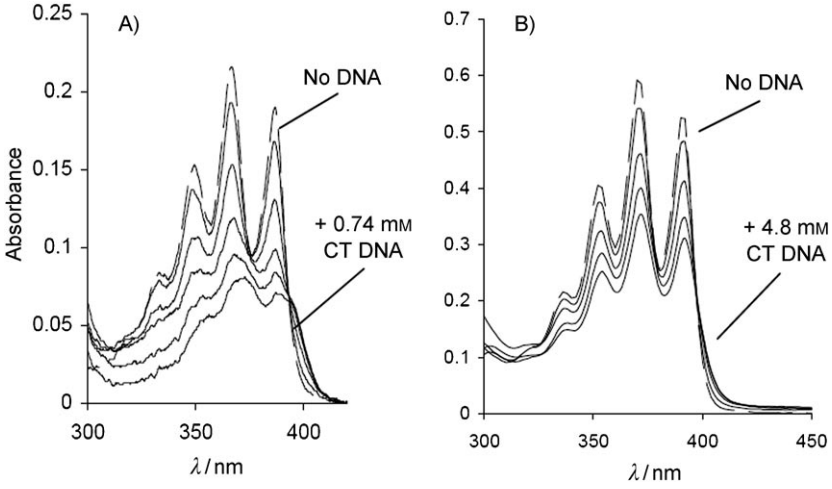


**Figure 1.** A) Absorption spectra of **L**[2] ($4.0\times10^{-5}$ M) in the presence of increasing concentrations of CT DNA (0, 0.04, 0.12, 0.28, 0.44, and 0.74 mM); B) Absorption spectra of complex **7** ($8.0\times10^{-5}$ M) in the presence of increasing concentrations of CT DNA (0, 0.16, 0.80, 1.76, and 4.80 mM).

The UV/vis spectroscopy data that were collected for **L**[1] and **L**[2] indicate that the binding of these probes to CT DNA is more likely to be by intercalation than groove binding because the spectral changes that arise from their interaction with CT DNA are in quite good agreement with the spectroscopic signatures that were assigned recently by Kumar et al.[13] These authors found a red shift, an extensive hypochromism and a substantial broadening of the bands of the anthracenyl chromophore in the 300–400 nm region, as a result of the strong electron interaction between the $\pi$ electrons of the intercalated polyaromatic structure and those of the DNA bases. In particular, the 5–6 nm red shifts of **L**[1] and **L**[2] compare well with the values (6–8 nm) that were reported in the literature for other (9-anthrylalkyl)amine derivatives, which are considered to act as DNA intercalators.[16] Nevertheless, we would like to emphasise that the UV/vis spectroscopy data that were obtained for **L**[1] and **L**[2] cannot completely exclude the possibility of groove binding; it is necessary to combine these data with the information that is provided by other spectroscopic techniques (see below) to draw more decisive conclusions. The UV/vis spectroscopy titration of complex **7** with CT DNA has shown that this compound is much less able to intercalate into the DNA compared to the respective ligand (**L**[2]). In a similar way, the UV/vis spectroscopy data that were obtained for the molecules that contain the anthracenyl fragment at the 4-position (**L**[3], **L**[4] and complex **9**) also indicated that these probes are unable to intercalate between the DNA base pairs.

398 nm for **7**. The presence of these isosbetic points indicates a smooth conversion of the free probes to the bound ones, as well as the prevalence of a dominant binding mode. The addition of DNA gives rise to the broadening of the vibronic structure of the anthracene absorption bands. This broadening is more intense for **L**[1] and **L**[2] than for **7** (Figure 1). The binding of these compounds to CT DNA is accompanied by a reduction in their extinction coefficients (hypochromism). This reduction varies between 45 and 66%, and is more pronounced for the ligands than for the Re complex (Table 1).

In comparison with the probes that have the terminal anthracenyl chromophore, the most striking difference in the spectral changes of the compounds that contain the 9-antrylmethyl group at the 4-position of the azole ring (**L**[3], **L**[4] and complex **9**) is the negligible or absent red shifts ($<0.5$ nm) of the respective absorption peaks, as exemplified for **L**[4] and **9** in Figure 2. The lack of broadening of these peaks is another feature of the spectra of **L**[3], **L**[4] and **9**. Unlike **9**, the hypochromism of **L**[3] (34% at 368 nm) and **L**[4] (33% at 367 nm) is significantly lower than the hypochromism (45–66%) that was observed for the compounds that bear the terminal anthracenyl group (Table 1).

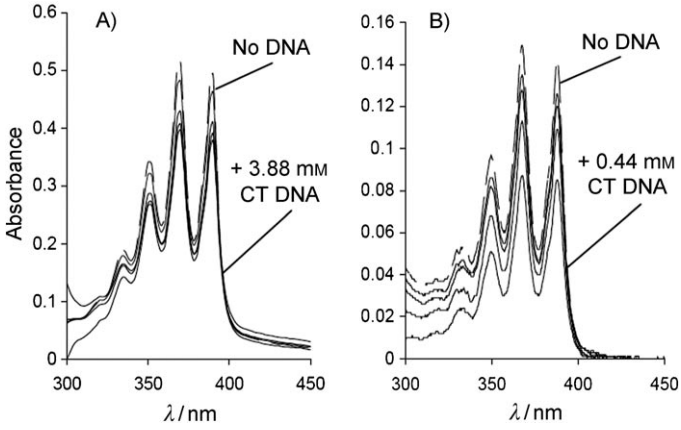


**Figure 2.** A) Absorption spectra of **L**[4] ($4.0\times10^{-5}$ M) in the presence of increasing concentrations of CT DNA (0, 0.64, 2.48, 3.44, and 3.88 mM); B) Absorption spectra of complex **9** ($4.0\times10^{-5}$ M) in the presence of increasing concentrations of CT DNA (0, 0.04, 0.08, 0.12, and 0.16 mM).

  

The UV/vis titration data were used to estimate the intrinsic binding constants ($K_b$) for all the evaluated compounds (**L**$^1$–**L**$^4$, **7** and **9**). To obtain the binding constants, the spectral data were fitted to a simple Scatchard model by using Equation (1) (see the Experimental Section).[17] The values that were obtained spanned between $(2.20\pm0.01)\times10^3\,M^{-1}$ and $(1.95\pm0.01)\times10^4\,M^{-1}$ (Table 1) and indicated that these compounds have a moderate affinity to CT DNA. As a general trend, we can say that the compounds that contain the terminal anthracenyl group (**L**$^1$, **L**$^2$ and **7**) have a smaller affinity to DNA than those that bear the same polyaromatic structure at the 4-position of the pyrazolyl ring (**L**$^3$, **L**$^4$ and **9**). From all the probes that were evaluated, complex **9** showed the highest constant, while complex **7** displayed the lowest one. This means that there is no well-defined tendency upon the introduction of the *fac*-$[Re(CO)_3]^+$ unit in terms of the DNA affinity of these two families of pyrazole–diamine ligands.

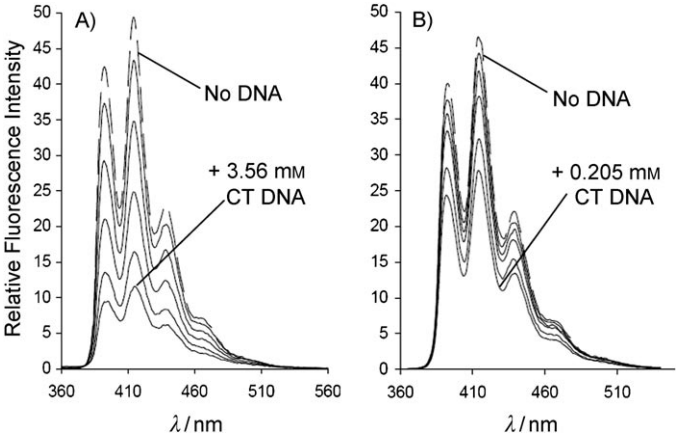


**Figure 4.** A) Fluorescence spectra of **L**$^4$ ($2.7\times10^{-5}$ M) in the presence of increasing concentrations of CT DNA (0, 0.11, 0.57, 1.32, 2.51, and 3.56 mM); B) Fluorescence spectra of complex **9** ($2.0\times10^{-5}$ M) in the presence of increasing concentrations of CT DNA (0, 0.009, 0.040, 0.060, 0.076, 0.205 mM).

### Fluorescence studies

The fluorescence intensity of all probes decreased rapidly with increasing concentrations of CT DNA, as shown in Figures 3 and 4. These changes in the emission spectra show that there

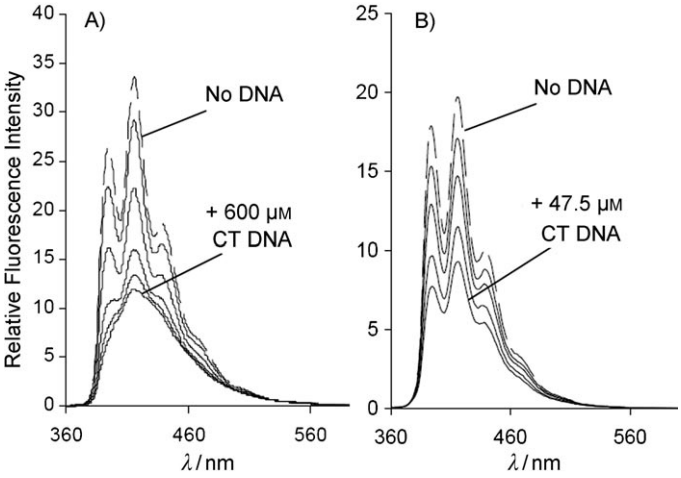


**Figure 3.** A) Fluorescence spectra of **L**$^2$ ($4.0\times10^{-5}$ M) in the presence of increasing concentrations of CT DNA (0, 40, 120, 280, 440, and 600 μM); B) Fluorescence spectra of complex **7** ($8.0\times10^{-6}$ M) in the presence of increasing concentrations of CT DNA (0, 4, 12, 24, and 47.5 μM).

is a strong quenching of the fluorescence of the compounds, as is commonly observed for anthryl probes.[16,18] As exemplified for **L**$^2$ in Figure 3, the spectra of the ligands with terminal 9-anthracenylmethyl groups **L**$^1$ and **L**$^2$ are considerably broadened at high DNA concentrations. Most probably, this broadening is a consequence of the superposition of the spectra from the bound and free chromophores, which are slightly shifted in wavelength from each other. This is consistent with the red shifts (5–6 nm) that were observed in the absorption spectra of these ligands and reflects the decrease in the HOMO–LUMO energy gap for the bound probes. Due to weaker or non-existent red shifts, the broadening of the emission spectra of the other compounds (**L**$^2$, **L**$^4$, **7** and **9**) is less evident (Figures 3 and 4).

To estimate the intrinsic binding constants, the fluorescence titration data were fitted with the noncooperative model of McGhee and von Hippel by using Equation (3) (see the Experimental Section).[19] An acceptable fit to this model was only obtained for the ligands pz*NN-Ant (pz* = pz, **L**$^1$; 3,5-$Me_2$pz, **L**$^2$). For the other compounds, the model was unreliable; this might indicate heterogeneous binding to DNA and/or the need to consider cooperativity.[20] The best linear fit to the binding isotherms that were constructed from the plot of $r/C_F$ versus $r$ (Figures S11 and S12 in the Supporting Information) led to binding constants of $(1.08\pm0.03)\times10^4$ and $(1.29\pm0.01)\times10^4\,M^{-1}$ for **L**$^1$ and **L**$^2$, respectively. From this fit, the binding site sizes ($n$) in base pairs that were obtained for **L**$^1$ ($n=2.7$) and **L**$^2$ ($n=2.1$) are compatible with the nearest-neighbour exclusion model, and are comparable to the values that were found for other amine derivatives of anthracene.[21,22] The binding constants that were obtained by the McGhee and von Hippel formalism are larger than the values of $4.25\times10^3\,M^{-1}$ (**L**$^1$) and $3.46\times10^3\,M^{-1}$ (**L**$^2$) that were obtained by the simplest Scatchard analysis. However, these differences can be considered to be acceptable within the experimental error that is inherent to the two different methods. Moreover, the values that were obtained by the two methods are consistent in the sense that both confirm that the presence of the methyl substituents at the 3 and 5-positions of the azole have a small influence on the DNA affinity.

### Induced Circular Dichromism (ICD) studies

None of the isolated compounds (**L**$^1$–**L**$^4$, **7** and **9**) that were evaluated in the DNA-binding studies has a CD spectrum. This is in agreement with the expected non-chirality of these molecules. However, their association with the right-handed DNA helix was expected to give ICD spectra in the 320–400 nm region where the anthracenyl chromophore absorbs. For an-

  

thracenyl derivatives, the ICD spectra of intercalated or groove-bound probes are expected to be different and, therefore, this technique can be useful to distinguish between different binding modes. Positive and intense ICD spectra are expected in the 320–400 nm region when the anthracenyl chromophore is intercalated with its long axis aligned to the long axis of the DNA base pairs.[13]

The pyrazolyl–diamine derivatives that have the terminal 9-anthrylmethyl substituent, pz*NN-Ant (pz* = pz, $L^1$; 3,5-$Me_2$pz, $L^2$) and *fac*-[Re(CO)$_3${3,5-$Me_2$pzNN-Ant}]Br (**7**), showed relatively intense positive ICD peaks in the 320–400 nm region upon binding to DNA, as shown for $L^2$ and for the respective Re complex (**7**) in Figure 5. However, the spectra of $L^1$ and $L^2$

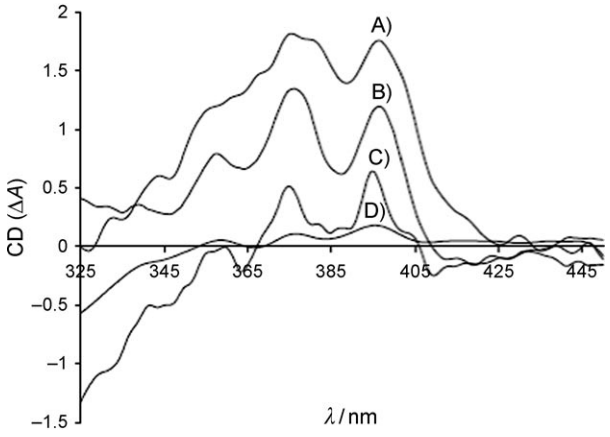


**Figure 5.** ICD spectra of the ligands $L^2$ and $L^4$, and their respective Re complexes, **7** and **9** at high ratios of CT DNA/probe concentrations: A) **7** ($8\times10^{-5}$ M) at a 18:1 molar ratio; B) $L^2$ ($5.3\times10^{-5}$ M) at a 13:1 molar ratio; C) $L^4$ ($10\times10^{-5}$ M) at a 60:1 molar ratio; D) **9** ($8.0\times10^{-5}$ M) at a 20.1 molar ratio.

emerged at lower [DNA]/[probe] ratios when compared with complex **7**. These data are consistent with the positive ICD spectra that were recently reported for other amine derivatives of anthracene that have been recognised as DNA intercalators.[13,16,23]

In contrast, the molecules that contain the anthracenyl chromophore at the 4-position of the pyrazole ring, Ant-pz*NN (pz* = pz, $L^3$; 3,5-$Me_2$pz, $L^4$) and *fac*-[Re(CO)$_3${Ant-3,5-$Me_2$-pzNN}]Br (**9**) showed much weaker ICD spectra even in the presence of a large excess of DNA ([DNA]/[probe] > 20:1). As an example, the ICD spectra that were obtained for $L^4$ and complex **9** are presented in Figure 5. This behaviour resembles that which was reported recently by Kumar et al. for an anthracenyl derivative that bore 2-hydroxyethylamine substituents at the 9- and 10-positions, a compound that has been proposed to be more likely to be bound to DNA through a groove-binding mode.[21]

### Linear dichromism (LD) studies

LD spectroscopy has been considered to be an excellent tool to distinguish the different DNA-binding modes for anthracenyl-containing probes. This technique provides more conclusive data than other spectroscopic techniques to assess the orientation of the chromophore with respect with the axis of the helix.[13,24] With the goal of confirming the above-discussed results for UV/visible, fluorescence and ICD spectroscopy studies, we evaluated the interaction of ligands $L^2$ and $L^4$ and their respective Re complexes (**7** and **9**) with CT DNA by LD spectroscopy. By studying only these compounds, we have taken into consideration that the presence of the methyl groups at the 3- and 5-positions of the azole does not significantly affect the affinity to DNA, and the binding modes, as well as the fact that it was not possible to evaluate the Re complexes of $L^1$ and $L^3$, as discussed above.

In the intercalation of anthracene derivatives, the short and long axes of the rings are oriented perpendicular to the DNA helix and this should result in negative LD signals at both absorption regions (230–300 nm and 300–450 nm) of the probe.[13] As shown in Figure 6, 3,5-$Me_2$pzNN-Ant ($L^2$) presents a negative LD band in the chromophore absorption region (300–450 nm); this suggests that the intercalation binding

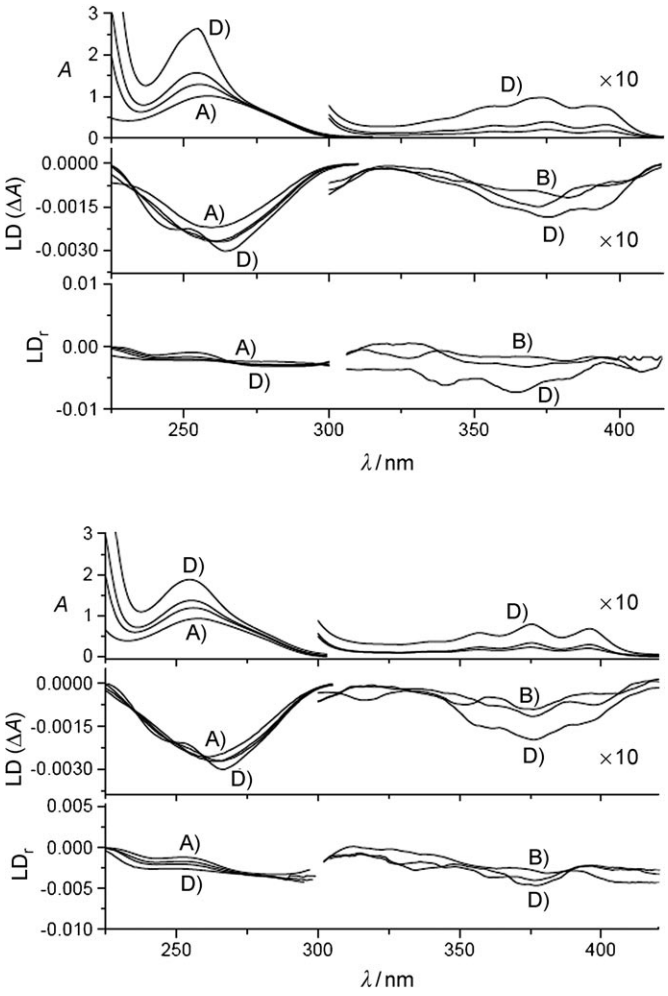


**Figure 6.** Absorption (upper panels), linear dichroism (LD, middle panels) and reduced linear dichroism (LD$_r$, lower panels) of $L^2$ (top) and complex **7** (bottom) at different [DNA]/[probe] molar ratios: A) no probe; B) 25; C) 12; D) 5. Spectra were recorded in 10 mM phosphate buffer at pH 7.2.

  

mode is dominant for this compound. The reduced LD spectrum ($LD_r = LD/A_{iso}$; Figure 6, lower panels) provides further information on the average orientation of the transition moment of $\mathbf{L^2}$ relative to those of the DNA bases, and it allows one to discriminate between homogeneous and heterogeneous binding. A nearly constant value of $LD_r$ over the range 310–450 nm was observed; this confirms the intercalation of $\mathbf{L^2}$ into the DNA. The ligand $\mathbf{L^2}$ induces an increase in the intensity of the LD DNA band (230–300 nm), which indicates that the DNA became more oriented upon the binding of $\mathbf{L^2}$. At the highest loading of $\mathbf{L^2}$ ([DNA]/[probe] = 5:1), there is a distortion of the band, which is probably due to external stacking of $\mathbf{L^2}$ onto the exterior of the helix. The corresponding Re complex, *fac*-[$Re(CO)_3${3,5-$Me_2$pzNN-Ant}]Br (**7**), also displays relatively intense LD peaks in the chromophore region, but this compound does not induce a large stiffening of the DNA because the measured LD values in the 230–300 nm region did not increase significantly compared to those of DNA alone (Figure 6). This indicates that the plane of the anthracene chromophore is tilted with respect to that of the DNA bases, and therefore, the complex seems to be only partially intercalated into the DNA. At any rate, the negative LD signals in the long-wavelength regions (300–450 nm) indicate that the transition dipole moment, and thus the $\pi$-systems of **7** is almost coplanar to the ones of the nucleic bases upon binding to the DNA; this was also confirmed by the analysis of the $LD_r$ spectrum.

As seen in Figure 7, we did not observe any LD signal in the chromophore-absorption region for Ant-3,5-$Me_2$pzNN ($\mathbf{L^4}$) and *fac*-[$Re(CO)_3${Ant-3,5-$Me_2$pzNN}]Br (**9**). This probably means that the compounds are not intercalated between the DNA base pairs. Alternatively, such behaviour could be justified by the very low binding affinities of these compounds. However, this seems not to be the case because the intrinsic binding constants ($K_b$) of $\mathbf{L^4}$ and **9** are larger then those of $\mathbf{L^2}$ and **7**, which displayed relatively intense LD signals in the chromophore region.

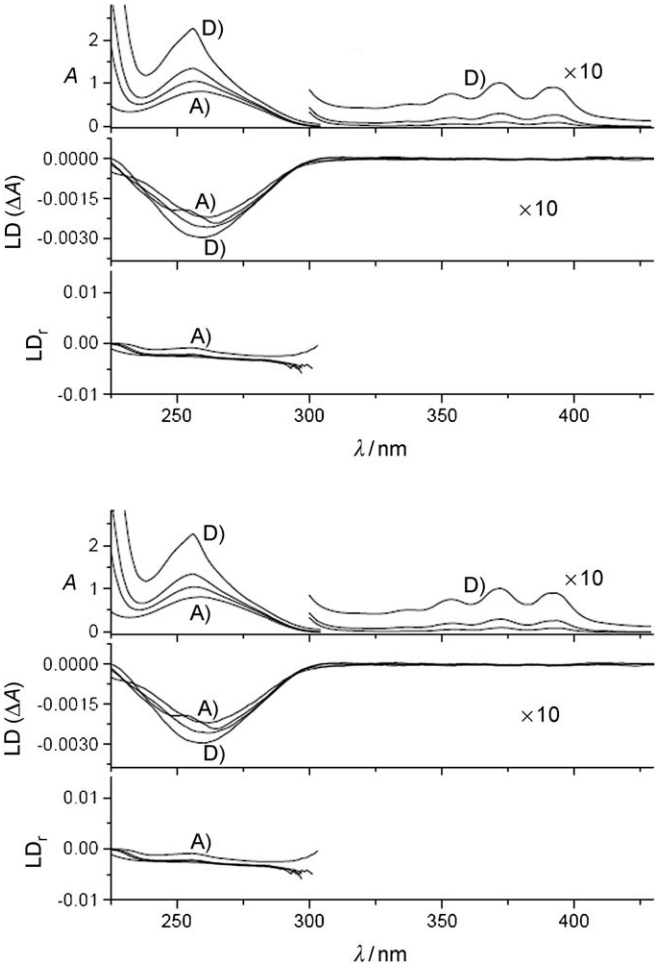


**Figure 7.** Absorption (upper panels), Linear dichroism (LD , middle panels) and reduced linear dichroism (LDr lower panels) of $\mathbf{L^4}$ (top) and complex **9** (bottom) at different [DNA]/[probe] molar ratios: A) no probe; B) 25; C) 12; D) 5. Spectra were recorded in 10 mM phosphate buffer at pH 7.2.

### Cell-uptake studies

In the design of $^{99m}$Tc radiopharmaceuticals, the ability to follow the trafficking and fate of the compounds at the cellular and subcellular level in real time is highly desirable. However, this is not achievable with the radioactive probes ($^{99m}$Tc), which are more adequate to obtain scintigraphic images from tissues and organs inside the body. By profiting from the similarities between the chemistry of Re and Tc, fluorescent probes that are based on organometallic $Re^I$ complexes emerged recently as an attractive alternative to bridge this gap between in vitro fluorescence-imaging studies and in vivo radioimaging.[25]

As stated in the introductory part of the paper, we intended to prove that the intrinsic fluorescence of anthracenyl chromophores, which were introduced at different positions of the framework of pyrazolyl–diamine chelators should enable us to image the intracellular localisation of their $Re^I$–tricarbonyl complexes. To confirm this possibility, we studied the cell uptake of the two Re complexes, *fac*-[$Re(CO)_3${3,5-$Me_2$pzNN-Ant}]Br (**7**) and *fac*-[$Re(CO)_3${Ant-3,5-$Me_2$pzNN}]Br (**9**), for which the DNA-binding properties have been evaluated. This was done by using fluorescence microscopy and B16-F1 murine melanoma cells. As depicted in Figure 8, complexes **7** and **9** were both detected (as blue fluorescence) inside the cells, with a significant accumulation in the nucleus (especially in the nucleoli), as confirmed by the simultaneous DRAQ5 labelling of DNA (Figure 8, arrows in top panels).

Like **7** and **9**, the respective ancillary ligands 3,5-$Me_2$pzNN-Ant $\mathbf{L^2}$, and Ant-3,5-$Me_2$pzNN, $\mathbf{L^4}$ were also able to enter the cells, but accumulated almost exclusively in the cytosol (Figure 8, bottom panels). Interestingly, this behaviour parallels the one that has been recently described for a cationic organometallic $Ru^{II}$ complex that contains a *N*-(anthracen-9-yl)imidazole co-ligand, for which the presence of the $Ru^{II}$ fragment also enhanced the nucleus uptake of the compounds.[26]

## Conclusions

We have shown that the position that is used to introduce a 9-anthrylmethyl group in the framework of pyrazolyl–diamine ligands has a crucial influence on the DNA-binding mode of the

  

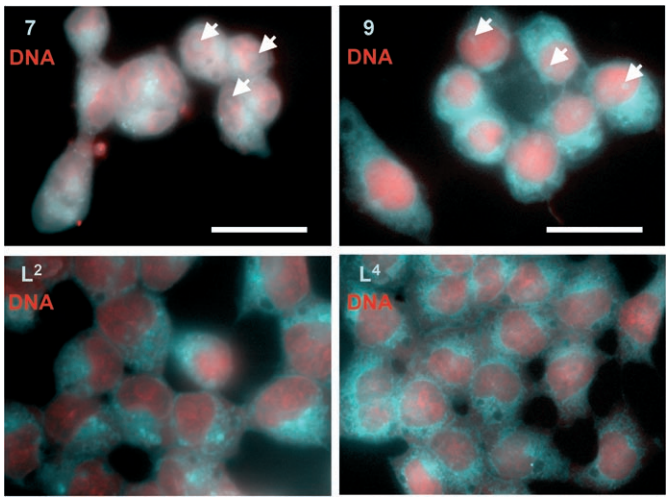


**Figure 8.** Fluorescence microscopy images of B16-F1 melanoma cells after 3 h of exposure to 80 μM of complexes **7** or **9** (cyan colour in left and right top panels, respectively) and compounds $L^2$ or $L^4$ (cyan colour in left and right bottom panels, respectively), followed by fixation and DNA staining with DRAQ5 (red colour in all panels), as described in the Experimental Section. The detection of blue fluorescence in the cells reveals that complexes **7** and **9** entered the cytoplasm and nucleus, and frequently accumulated in the nucleoli (white arrows). Compounds $L^2$ and $L^4$, on the other hand, accumulated in the cytoplasm and did not significantly target the nucleus, as evaluated by the lack of blue fluorescence in cells' nuclei (bottom panels, cyan colour). White bar = 20 μm.

compounds. Different spectroscopic techniques (UV/vis, fluorescence, CD, LD) consistently demonstrated that the ligands that have a terminal 9-anthrylmethyl group, pz*NN-Ant (pz* = pz, $L^1$; 3,5-$Me_2$pz, $L^2$) probably intercalate into the DNA helix. To the contrary, the ligands that contain the same polyaromatic group at the 4-position of the azole ring, Ant-pz*NN (pz* = pz, $L^3$; 3,5-$Me_2$pz, $L^4$) act more like groove binders. This difference is certainly due to the steric requirements of the pyrazolyl ring, which, because it is closer to the anthracenyl chromophore in $L^3$ and $L^4$, hinders its intercalation. Similar effects have been reported for other anthracene derivatives with bulky substituents at the 9 or 10-positions.[13,22]

The introduction of the 9-anthrylmethyl group in the framework of pyrazolyl–diamine chelators did not compromise their coordination capability towards the *fac*-$[Re(CO)_3]^+$ moiety. Surprisingly, the substituents (H vs. Me) at the 3 and 5-positions of the pirazolyl ring had a strong influence on the formation of different diastereoisomers. Compound $L^1$ afforded a mixture of complexes, while $L^2$–$L^4$ led to the well-defined complexes *fac*-$[Re(CO)_3${3,5-$Me_2$pzNN-Ant}]Br (**7**) and *fac*-$[Re(CO)_3$-{Antpz*NN}]Br (pz* = pz, **8**; 3,5-$Me_2$pz, **9**) which were fully characterised. The evaluation of the DNA-binding properties of **7** and **9** showed that these compounds follow the trend that was observed for the corresponding ligands, that is, the molecules with the 9-anthrylmethyl substituent at the 4-position of the azolyl ring (**9**) tend to act as groove binders, while those with a terminal anthracenyl group (**7**) are better able to intercalate into the DNA helix.

Regardless of the mode of interaction with DNA, complexes **7** and **9** can reach the nucleus of murine B16-F1 cells, as demonstrated by fluorescence microscopy. In contrast, the respective free ligands ($L^2$ and $L^4$) accumulate preferentially on the cytosol of the same cell line. Although in the case of $L^2$, the inclusion of the organometallic fragment decreases the ability of the compounds to intercalate into DNA; it also seems to facilitate the nuclear uptake of the compounds. Currently, we are studying the possibility of preparing the $^{99m}$Tc congeners of **7** and **9**. We expect that the radioactive complexes will also accumulate in the cell nucleus, and will induce enhanced DNA damage, which is a crucial issue for potential radiotherapy with $^{99m}$Tc radiopharmaceuticals.

## Experimental Section

**General procedures**: The synthesis of the ligands and complexes was carried out under a nitrogen atmosphere by using standard Schlenk techniques and dry solvents, but the work-up was performed under air. The compounds 9-bromomethylanthracene,[27] 2-(9-antrylmethyl)propane-1,3-diol,[28] *N*$^1$-[2-(3,5-dimethyl-1*H*-pyrazol-1-yl)ethyl]ethane-1,2-diamine,[8] *N*$^1$-[2-(1*H*-pyrazol-1-yl)ethyl]ethane-1,2-diamine,[10] $[Re(CO)_5Br]$[29] and $(NEt_4)_2[Re(CO)_3Br_3]$[30] were prepared by the literature methods. $^1$H and $^{13}$C NMR spectra were recorded on a Varian Unity 300 MHz spectrometer; $^1$H and $^{13}$C chemical shifts are given in ppm and were referenced with the residual solvent resonances relative to $SiMe_4$. IR spectra were recorded as KBr pellets on a Bruker, Tensor 27 spectrometer. All the new ligands, $L^1$–$L^4$, were characterised by Fourier transform ion cyclotron resonance mass spectrometry (FT/ICR-MS) with electron impact ionisation on an Extrel FTMS 2001-DT instrument. Electrospray mass spectrometry measurements (ESI-MS) were performed for the Re complexes (**7**–**9**) on a ThermoFinnigan LCQ mass spectrometer in positive-ion mode. Thin layer chromatography (TLC) was done by using plates from Merck (Silica gel 60 F254). Column chromatography was performed on silica gel 60 (Merck).

### Syntheses of the ligands

*Pz($CH_2$)$_2$NH($CH_2$)$_2$NH$CH_2$-9-anthryl ($L^1$)*: Solid 9-anthracenealdehyde (86 mg, 1.25 mmol) was added to a solution of *N*$^1$-[2-(1*H*-pyrazol-1-yl)ethyl]ethane-1,2-diamine (193 mg, 1.25 mmol) and $NEt_3$ (253 mg, 2.5 mmol) in MeOH/$CH_2Cl_2$ (1:3, 20 mL), and the resulting mixture was stirred overnight at room temperature. Then $NaBH_4$ (0.032 g, 0.834 mmol) was added, and the mixture allowed to react for a further 24 h. The solution was then washed with a sat. $K_2CO_3$ solution, and the organic layer was separated and dried over $MgSO_4$. Removal of the solvent under vacuum yielded an oily residue, which was purified by silica gel column chromatography by using a gradient elution from dichloromethane to methanol, and finally to methanol/ammonia (8:2). Removal of the solvent from the collected fractions yielded a dark-orange oil; yield: 54 mg, 0.14 mmol (34%). $^1$H NMR ($CDCl_3$): $\delta$ = 8.37 (s, 1H; Ar), 8.30 (d, 2H; Ar), 7.98 (d, 2H; Ar), 7.48 (m, 5H; Ar + H-3/5 (pz)), 7.29 (d, 1H; H-3/5 (pz)), 6.13 (t, 1H; H-4 (pz)), 4.68 (s, 2H; $CH_2$,), 4.12 (t, 2H; $CH_2$), 2.93 (m, 4H; $CH_2$), 2.73 ppm (t, 2H; $CH_2$); $^{13}$C NMR ($CDCl_3$): $\delta$ = 139.4 (C-3 (pz)), 131.4 (C-5 (pz)), 130.1 (Ar), 129.5 (Ar), 129.0 (Ar), 127.1 (Ar), 126.0 (Ar), 124.8 (Ar), 124.0 (Ar), 105.2 (C-4 (pz)), 51.8 ($CH_2$), 49.2 ($CH_2$), 49.0 ($CH_2$), 48.7 ($CH_2$), 45.4 ppm ($CH_2$). FT/ICR-MS: *m/z*: 345.2 $[M+H]^+$.

*3,5-$Me_2$pz($CH_2$)$_2$NH($CH_2$)$_2$NH$CH_2$-9-anthryl ($L^2$)*: Compound $L^2$ is a yellow solid that was prepared as described above for $L^1$ by reacting *N*$^1$-[2-(3,5-dimethyl-1*H*-pyrazol-1-yl)ethyl]ethane-1,2-diamine (181 mg, 0.88 mmol) with 9-anthracenealdehyde (160 mg,

  

0.88 mmol), but without using $NEt_3$. The purification of $L^2$ was accomplished by silica gel column chromatography by using a gradient elution from dichloromethane to methanol; yield: 277 mg, 0.75 mmol (85%). $^1$H NMR ($CDCl_3$): $\delta = 8.37$ (s, 1H; Ar), 8.29 (d, 2H; Ar), 7.97 (d, 2H; Ar), 7.48 (m, 4H; Ar), 5.68 (s, 1H; H-4 (pz)), 4.69 (s, 2H; $CH_2$,), 3.95 (t, 2H; $CH_2$), 2.92 (m, 4H; $CH_2$), 2.75 (t, 2H; $CH_2$), 2.14 (s, 3H; $CH_3$), 2.10 ppm (s, 3H; $CH_3$); $^{13}$C NMR ($CDCl_3$): $\delta = 147.0$ (C-3 (pz)), 138.6 (C-5 (pz), 131.1 (Ar), 129.9 (Ar), 128.7 (Ar), 126.7 (Ar), 125.6 (Ar), 124.9 (Ar), 124.5 (Ar), 123.8 (Ar), 104.4 (C-4 (pz)), 49.2 ($CH_2$), 48.8 ($CH_2$), 48.6 ($CH_2$), 48.0 ($CH_2$), 45.2 ($CH_2$), 13.1 ($CH_3$), 10.6 ppm ($CH_3$). FT/ICR-MS: *m/z*: 373.2 $[M+H]^+$.

*2-(9-Anthrylmethyl)propane-1,3-dialdehyde (**1**)*: DMSO (3.6 mL, 3.3 mmol) and $NEt_3$ (4.53 mL, 32.74 mmol) were added to a solution of 2-(9-anthrylmethyl)propane-1,3-diol (880 mg, 3.3 mmol) in $CH_2Cl_2$, while keeping the temperature at 0 °C. Then, pyridine·$SO_3$ (2.57 g, 16.16 mmol) was slowly added to the mixture. After complete addition, the reaction was warmed to RT and stirred overnight. After washing with diethyl ether, the mixture was diluted with $CHCl_3$ (100 mL), and the organic layer was washed with distilled water. The organic layer was separated, dried over $MgSO_4$ and concentrated under vacuum to afford compound **1** as a yellow oil; yield: 468 mg, 1.78 mmol (54%). $^1$H NMR ($CDCl_3$): $\delta =$ 13.60 (sbr, 1H; OH), 8.43 (s, 1H; Ar), 8.14 (m, 4H; Ar + $CH_2$), 8.02 (d, 2H; Ar), 7.50 (m, 4H; Ar), 4.53 ppm (s, 2H; $CH_2$).

*2-(9-Anthrylmethyl)pentane-2,4-dione (**2**)*: Acetylacetone (0.242 mL, 2.34 mmol) was added to a suspension of NaH (62 mg, 2.58 mmol) in THF, and the mixture stirred for 2 h at RT. After cooling to 0 °C, solid 9-bromomethylanthracene (634 mg, 2.34 mmol) was slowly added, and the resulting mixture was stirred overnight at RT. After the addition of of aqueous 1 N HCl (60 mL) at 0 °C, the product was extracted with diethyl ether. Removal of the solvent gave compound **2** as a yellow oil; yield: 523 mg, 1.80 mmol (77%). $^1$H NMR ($CDCl_3$): $\delta = 8.34$ (s, 1H; Ar), 8.14 (d, 2H; Ar), 7.98 (d, 2H; Ar), 7.49 (m, 4H; Ar), 4.23 (t, 1H; CH), 4.14 (d, 2H; $CH_2$), 1.93 ppm (s, 6H; $CH_3$).

*4-(9-Anthrylmethyl)pz($CH_2$)$_2$OH (**3**)*: 2-Hydroxyethylhydrazine (120 μL, 1.79 mmol) dissolved in ethanol (20 mL) was added dropwise to a solution of compound **1** (468 mg, 1.79 mmol) in $CHCl_3$/EtOH (1:1, 20 mL), while keeping the temperature at 0 °C. After complete addition, the mixture was stirred at RT for 1 h. The solvent was removed under vacuum and the residue was purified by silica gel chromatography by using a gradient elution from $CH_2Cl_2$ to $CH_2Cl_2$/MeOH (8:2). Compound **3** was recovered as a yellow oil after removal of the solvent from the collected fractions; yield: 468 mg, 1.78 mmol (54%). $^1$H NMR ($CDCl_3$): $\delta = 8.46$ (s, 1H; Ar), 8.31 (d, 2H; Ar), 8.09 (d, 2H; Ar), 7.51 (m, 4H; Ar), 7.54 (s, 1H; H-3/5 (pz)), 6.97 (s, 1H; H-3/5 (pz)), 4.80 (s, 2H, $CH_2$), 3.99 (t, 2H; $CH_2$), 3.81 ppm (t, 2H; $CH_2$).

*3,5-$Me_2$-4-(9-anthrylmethyl)pz($CH_2$)$_2$OH (**4**)*: Compound **4** is a yellow oil that was prepared and recovered as described above for **3**, by the reaction of 2-hydroxyethylhydrazine (50 μL, 0.72 mmol) and compound **2** (209 mg, 0.72 mmol). The purification of **4** was done by silica gel chromatography by using a gradient elution from $CH_2Cl_2$ to MeOH; yield: 127 mg, 1.78 mmol (62%). $^1$H NMR ($CDCl_3$):$\delta = 8.40$ (s, 1H; Ar), 8.12 (d, 2H; Ar), 8.02 (d, 2H; Ar), 7.36 (m, 4H; Ar), 4.69 (s, 2H; $CH_2$), 3.94 (m, 4H; $CH_2$), 1.89 (s, 3H; $CH_3$), 1.60 ppm (s, 3H; $CH_3$).

*4-(9-Anthrylmethyl)pz($CH_2$)$_2$Br (**5**)*: $PBr_3$ (336 μL, 3.57 mmol) was added to a solution of compound **3** (539 mg, 1.79 mmol) in toluene, and the resulting mixture was refluxed overnight. After cooling to room temperature, the toluene solution was successively washed with sat. aq $NaHCO_3$ and distilled water. The organic layer was dried over $MgSO_4$ and the solvent was removed under vacuum to afford compound **5** as an orange oil; yield: 553 mg, 1.51 mmol (84%). $^1$H NMR ($CDCl_3$): $\delta = 8.39$ (s, 1H; Ar), 8.22 (d, 2H; Ar), 8.01 (d, 2H; Ar), 7.46 (m, 4H; Ar), 7.43 (s, 1H; H-pz), 6.92 (s, 1H; H-pz), 4.76 (s, 2H; $ArCH_2$), 4.24 (t, 2H; $CH_2$), 3.56 ppm (t, 2H; $CH_2$).

*3,5-$Me_2$-4-(9-anthrylmethyl)pz($CH_2$)$_2$Br (**6**)*: Compound **6** is an orange oil that was prepared as described above for **5**, by starting from **4** (127 mg, 0.35 mmol); yield: 77% (105 mg, 0.27 mmol). $^1$H NMR ($CDCl_3$): $\delta = 8.39$ (s, 1H; Ar), 8.12 (d, 2H; Ar), 7.99 (d, 2H; Ar), 7.44 (m, 4H; Ar), 4.65 (s, 2H; Ar), 4.24 (t, 2H; $CH_2$), 3.59 (t, 2H; $CH_2$-pz), 1.87 (s, 3H; $CH_3$), 1.65 ppm (s, 3H; $CH_3$).

*4-(9-Anthrylmethyl)pz($CH_2$)$_2$NH($CH_2$)$_2$$NH_2$ ($L^3$)*: A solution of compound **5** (553 mg, 1.51 mmol) in methanol was slowly added to a solution of ethylenediamine (2 mL, 30 mmol) in the same solvent. After complete addition, the resulting mixture was refluxed overnight. The solvent was removed under vacuum and the residue was dissolved in chloroform and washed several times with distilled water. The organic layer was separated, dried over $MgSO_4$, concentrated under vacuum and purified by column chromatography (silica gel, by gradient elution $CH_2Cl_2$/MeOH 95:5 to $CH_2Cl_2$/MeOH/$NH_4OH$ 60:40:4) to give an orange-yellow oil; yield: 39% (204 mg, 0.59 mmol). $^1$H NMR ($CDCl_3$): $\delta = 8.35$ (s, 1H; Ar), 8.22 (d, 2H; Ar), 7.98 (d, 2H; Ar,) 7.44 (m, 4H; Ar), 7.38 (s, 1H; H3/5-pz), 6.84 (s, 1H, (H-pz)), 4.72 (m, 2H; Ar-$CH_2$,), 3.94 (t, 2H; $CH_2$,) 2.84 (t, 2H; $CH_2$), 2.58 (t, 2H; $CH_2$), 2.47 ppm (brt, 3H; $CH_2$, NH); $^{13}$C NMR ($CDCl_3$): $\delta = 138.7$ (C-3, (pz)), 132.2 (C-5, pz), 131.6 (Ar), 129.6 (ArH), 129.1 (Ar), 128.5 (Ar), 126.2 (Ar), 125.7 (Ar), 124.9 (Ar), 124.5 (Ar), 120.5 (C-4 (pz), 51.8 ($CH_2$), 51.6 ($CH_2$), 49.0 ($CH_2$), 41.3 ($CH_2$), 22.9 ppm ($CH_2$). FT/ICR-MS: (*m/z*): 345.2 $[M+H]^+$ .

*3,5-$Me_2$-4-(9-anthrylmethyl)pz($CH_2$)$_2$NH($CH_2$)$_2$$NH_2$ ($L^4$)*: Compound $L^4$ was synthesised as described above for $L^3$, by starting from **6** (105 mg, 0.24 mmol) and ethylenediamine (320 μL, 4.8 mmol). $L^4$ was obtained as an orange oil after purification by silica gel chromatography by using a gradient elution from MeOH to MeOH/$NH_4OH$ (8:2); yield: 45 mg, 0.12 mmol, (50%). $^1$H NMR ($CDCl_3$): $\delta =$ 8.39 (s, 1H; Ar), 8.15 (m, 2H; Ar), 8.00 (m, 2H; Ar), 7.42 (m, 4H; Ar), 4.65 (m, 2H; Ar), 3.94 (t, 2H; $CH_2$), 2.88 (t, 2H; $CH_2$), 2.66 (m, 2H; $CH_2$), 2.57 (m, 2H; $CH_2$), 1.89 (s, 3H; $CH_3$), 1.57 ppm (s, 3H, $CH_3$). $^{13}$C NMR ($CDCl_3$): $\delta = 146.0$ (C-3 (pz)), 136.0 (C-5 (pz)), 131.7 (Ar), 131.4 (Ar), 130.5 (Ar), 129.2 (Ar), 126.4 (Ar), 125.7 (Ar), 124.9 (Ar), 124.7 (Ar), 114.37 (C-4 (pz)), 52.0 ($CH_2$), 49.1 ($CH_2$), 48.3 ($CH_2$), 41.5 ($CH_2$), 23.5 ($CH_2$), 12.5 ($CH_3$), 9.5 ppm ($CH_3$). FT/ICR-MS: *m/z*: 373.2 $[M+H]^+$.

**Syntheses of the Re complexes**

*General procedure*: The complexes *fac*-[Re(CO)$_3${3,5-$Me_2$pz($CH_2$)$_2$NH-($CH_2$)$_2$NH$CH_2$-9-anthryl (**7**)) and *fac*-[Re(CO)$_3${pz*($CH_2$)$_2$NH($CH_2$)$_2$$NH_2$}] (pz* = 4-(9-anthrylmethyl)pz (**8**), 3,5-$Me_2$-4-(9-anthrylmethyl)pz (**9**)) were prepared by overnight reaction of [Re(CO)$_5$Br] with an equimolar amount of the respective ligand ($L^2$–$L^4$) in refluxing methanol.

fac-*[Re(CO)$_3${3,5-$Me_2$pz($CH_2$)$_2$NH($CH_2$)$_2$NH$CH_2$-9-anthryl}] (**7**)*: The synthesis of complex **7** was accomplished by following the general procedure, by using [Re(CO)$_5$Br] 132 mg (0.325 mmol) and $L^2$ (121 mg, 0.327 mmol). After removal of the solvent under vacuum, the crude was dissolved in the minimum volume of THF. Upon addition of *n*-hexane, a microcrystalline yellow solid precipitated. The precipitate was washed with THF and dried under vacuum; yield: 67 mg, 0.093 mmol (29%). $^1$H NMR ($CD_3OD$): $\delta = 8.67$ (s, 1H;

  

Ar), 8.41 (d, 2H; Ar), 8.15 (d, 2H; Ar), 7.70 (m, 2H; Ar), 7.57 (m, 2H; Ar), 7.18 (br s, 1H; NH), 6.09 (s, 1H; H-4 (pz)), 5.55 (m, 2H; $CH_2$,), 5.37 (m, 1H; $CH_2$), 4.50 (m, 1H; $CH_2$), 4.36 (br s, 1H; NH), 4.02 (m, 1H; $CH_2$), 3.52 (m, 1H; $CH_2$), 2.81 (m, 1H; $CH_2$), 2.62 (m, 2H; $CH_2$), 2.39 (m, 1H; $CH_2$), 2.28 (s, 3H; $CH_3$), 2.25 ppm (s, 3H; $CH_3$). $^{13}$C NMR ($CD_3OD$): $\delta = 152.5$ (C-3/5 (pz)), 144.1 (C-3,5 (pz)), 131.4 (Ar), 130.5 (Ar), 130.1 (Ar), 129.9 (Ar), 128.2 (Ar), 126.3 (Ar), 125.6 (Ar), 122.2 (Ar), 108.2 (C-4 (pz)), 53.2 ($CH_2$), 49.0 ($CH_2$), 48.6 ($CH_2$), 48.1 ($CH_2$), 15.4 ($CH_3$), 12.2 ppm ($CH_3$). IR (KBr, $\nu_{max}$): 2024s, 1900s cm$^{-1}$ (C≡O). ESI-MS: (*m/z*): 643.0 $[M]^+$.

fac-*[Re(CO)$_3${4-(9-anthrylmethyl)pz(CH$_2$)$_2$NH(CH$_2$)$_2$NH$_2$}]* (**8**): The synthesis of complex **8** was accomplished by following the general procedure, by using $[Re(CO)_5Br]$ (53 mg, 0.130 mmol) and $\mathbf{L^3}$ (45 mg, 0.130 mmol). After evaporation of the solvent, the crude was washed with chloroform, and the recovered yellow solid was dried under vacuum; yield: 50 mg, 0.072 mmol (55%). $^1$H NMR ($CD_3OD$): $\delta = 8.49$ (s, 1H; Ar,), 8.32 (d, 2H; Ar), 8.08 (d, 2H; Ar), 7.89 (s, 1H; H-3/5 (pz)), 7.47 (m, 4H; Ar), 7.38 (s, 1H; H-3/5 (pz)), 6.93 (br s, 1H; NH), 5.26 (br s, NH), 4.44 (m, 1H; $CH_2$), 4.31 (m, 1H; $CH_2$), 4.10 (m, 2H; $CH_2$), 3.41(br s; NH), 2.72 (m, 2H; $CH_2$), 2.42 (m, 4H; $CH_2$), 1.97 ppm (m, 1H; $CH_2$). $^{13}$C NMR ([D$_6$]DMSO): $\delta = 194.3$ (C=O), 144.0 (C-4 (pz)), 133.0 (Ar), 131.6 (Ar), 131.3 (Ar), 129.3 (Ar), 129.2 (Ar), 126.5 (Ar), 126.4 (Ar), 125.3 (Ar), 124.6 (C-3,5 (pz)), 121.9 (C-3/5 (pz)), 79.2 ($CH_2$), 54.7 ($CH_2$), 51.7 ($CH_2$), 47.8 ($CH_2$), 21.9 ppm ($CH_2$). IR (KBr, $\nu_{max}$): 2026s, 1896s cm$^{-1}$ (C≡O). ESI-MS (*m/z*): 614.9 $[M]^+$.

fac-*[Re(CO)$_3${3,5-Me$_2$-(9-anthrylmethyl)pz(CH$_2$)$_2$NH(CH$_2$)$_2$NH$_2$}* (**9**): The synthesis of complex **9** was accomplished by following the general procedure, by using $[Re(CO)_5Br]$ (108 mg, 0.266 mmol) and $\mathbf{L^3}$ (100 mg, 0.267 mmol). The solvent was removed under vacuum and the crude washed with n-hexane to afford complex **9** as a yellow solid; yield: 190 mg, 0.262 mmol (98%). $^1$H NMR ($CD_3OD$): $\delta = 8.49$ (s, 1H; Ar), 8.16 (d, 2H; Ar), 8.05 (d, 2H; Ar), 7.49 (m, 4H; Ar), 6.90 (br, 1H; NH), 5.38 (br s; NH), 4.60 (m, 1H; $CH_2$), 4.38 (m, 1H; $CH_2$), 4.02 (m, 2H; $CH_2$), 3.82 (br s, NH), 3.41 (m, 1H; $CH_2$), 2.84 (m, 2H; $CH_2$), 2.44 (m, 4H; $CH_2$), 2.22 (s, 3H; $CH_3$), 1.66 ppm (s, 3H; $CH_3$); $^{13}$C NMR ($CD_3OD$): $\delta = 194.5$ (C=O), 152.7 (C-3/5 (pz)), 142.3 (C-3/5 (pz)), 133.0 (Ar), 131.9 (Ar), 131.2 (Ar), 130.5 (Ar), 128.2 (Ar), 127.3 (Ar), 126.2 (Ar), 125.4 (Ar), 118.4 (C-4 (pz)), 55.7 ($CH_2$), 43.1 ($CH_2$), 30.7 ($CH_2$), 24.1 ($CH_2$), 14.9 ($CH_3$), 10.0 ppm ($CH_3$). IR (KBr, $\nu_{max}$): 2025s, 1889s cm$^{-1}$ (C≡O). ESI-MS (*m/z*): 643.0 $[M]^+$.

**DNA binding studies**: Calf thymus DNA (CT DNA) sodium salt was purchased from Sigma and was used without further purification. The DNA concentrations per nucleotide of stock solutions in Tris buffer (10 mM Tris, 50 mM NaCl, pH 7.4) were determined by absorption spectroscopy at 260 nm, after adequate dilution with the buffer and using the reported molar absorptivity of 6600 M$^{-1}$ cm$^{-1}$.[31]

The purity of the DNA samples was checked by monitoring the value of the $A_{260}/A_{280}$ ratio. All measurements that involved DNA and the different test compounds ($\mathbf{L^1}$–$\mathbf{L^4}$, **7** and **9**) were carried out in Tris buffer (10 mM Tris, 50 mM NaCl, pH 7.4) or in phosphate buffer (10 mM, pH 7.2) that contained a small amount of DMSO [5–10% (*v/v*)] due to the low solubility of the compounds in aqueous medium.

The absorption and fluorescence titrations were performed by keeping the concentration of the probe constant, while varying the concentration of DNA. The titration data were fitted to a simple Scatchard model, or to the McGhee–von Hippel site-exclusion model to obtain the intrinsic binding constant ($K_b$).[17,19] All calculations were done by considering the DNA concentration in base pairs, and the data were corrected for volume changes.

**Absorption spectroscopy:** UV/vis absorption spectra were recorded on Perkin–Elmer Lambda 9 or Jasco V560 spectrophotometers by using 1 cm path-length quartz cells. In order to eliminate any interference of the DNA absorbance in the region of the anthracenyl chromophore absorbance, an equal amount of CT DNA in Tris buffer was added to the sample and reference cells. After each addition of CT DNA, the solution was allowed to equilibrate and the absorption spectrum was recorded until there was no further absorbance decrease.

The absorption titration data were fitted to Equation (1),[17] where $D$ is the concentration of DNA in base pairs and $\Delta\varepsilon_{ap} = [\varepsilon_a - \varepsilon_F]$ and $\Delta\varepsilon = [\varepsilon_B - \varepsilon_F]$.

$$D/\Delta\varepsilon_{ap} = D/\Delta\varepsilon + 1/\Delta\varepsilon K_b \quad (1)$$

The apparent extinction coefficient, $\varepsilon_a$, is the ratio of the observed absorbance of the sample and the total concentration of the probe ($A_{obs}$/[probe]). $\varepsilon_B$ and $\varepsilon_F$ correspond to the extinction coefficients of the bound and free forms of the probe, respectively. The obtained $\varepsilon_B$ value was confirmed through an independent method, in which the absorbance was extrapolated from a linear plot of the absorbance *vs.* 1/[DNA] for [DNA] ≫ [probe]. The intrinsic binding constant ($K_b$) was determined from the plot of $D/\Delta\varepsilon_{ap}$ vs $D$.

**Fluorescence studies**: Fluorescence spectra were recorded in a Perkin–Elmer LS50B spectrofluorimeter with a sample holder thermostatted at 28 °C using a quartz cuvette of 1 cm. After each addition of CT DNA in Tris buffer, the solution was allowed to equilibrate for 2 min and absorption spectra were recorded in order to determine the absorbance values at the excitation wavelength. The fluorescence spectra were then recorded until there was no further decrease in the fluorescence intensity. Ligands $\mathbf{L^1}$ and $\mathbf{L^2}$ and complex **7** were excited at $\lambda = 340$ nm, while $\mathbf{L^3}$, $\mathbf{L^4}$ and complex **9** were excited at $\lambda = 345$ nm. Emission and excitation slits were chosen in order to maximise the fluorescence intensity. Emission spectra were recorded from $\lambda = 360$–600 nm, with a scan speed of 100 nm min$^{-1}$.

The fluorescent data were also used to determine the intrinsic binding constant ($K_b$) of the probes. The concentration of the free probe in each sample ($C_F$) was calculated according to Equation (2), where $C_T$ is the total concentration of the probe and P is the ratio of the observed quantum yield of the fluorescence of the bound probe to that of the free probe.[31]

$$C_F = C_T(I/I_0 - P)/(1 - P) \quad (2)$$

The value of $P$, which corresponds to the limiting fluorescence yield, is the $y$-intercept from the plot of $I/I_0$ vs. 1/[DNA], $I$ and $I_0$ are the fluorescence intensities of the probes in the presence or absence of DNA. The amount of bound probe ($C_B$) at any concentration is given by $C_T - C_F$. The binding constant ($K_b$) and the binding site size ($n$) in base pairs were obtained from the plot of $r/C_F$ vs. $r$, where $r = C_B$/[DNA], according to the McGhee–von Hippel Equation (3).[19]

$$r/C_F = K_b(1 - nr)[(1 - nr)/[1 - (n-1)r]]^{n-1} \quad (3)$$

**Circular dichroism (CD) studies**: The CD spectra were recorded at 28 °C on a Jasco J-720 spectropolarimeter with a UV/vis (200–700 nm) photomultiplier. Solutions of the probe and CT DNA in Tris buffer were placed in a 1 cm (or 2 cm) path-length quartz cell, and the spectra were recorded in the 250–500 nm region with subtraction of the buffer baseline. The following operating parameters were used to collect the CD spectra: bandwidth, 0.5 nm; sensitivity,

  

10 mdeg; resolution, 0.2 nm; scan speed, 50 nm min$^{-1}$; response time, 4 s; accumulations, 1.

**Linear dichroism (LD) studies**: The LD measurements were performed with a Jasco J500 A spectropolarimeter that was equipped with an IBM PC and a Jasco Jinterface. The studies were done with CT DNA in 10 mM phosphate buffer at pH 7.2, and the sample orientation was produced by a device that was designed by Wada and Kozawa for the studies of differential flow dichroism of polymer solution at a shear gradient of 700 rpm.[32] The reduced linear dichroism, was defined by the ratio ($LD_r = LD/A_{iso}$) between the LD values and the absorbance of the unoriented sample at rest ($A_{iso}$), which might be related to the orientation of DNA (S) and the angle between the respective light-absorbing transition moment and DNA helix axis according to Norden et al.[24]

**Cell uptake by fluorescence microscopy**: B16-F1 murine melanoma cells were grown at 37 °C in DMEM medium (GIBCO) that was supplemented with 10% fetal bovine serum, under a humidified 5% $CO_2$ atmosphere. For microscopy, cells were cultured overnight on coverslips that had been sterilised in ethanol, and then placed in sterile six-well plates in which ~$5\times10^4$ cells per well were plated. The next day the medium was discarded and replaced by fresh medium that contained ligand or complex (80 μM). The cells were then exposed to compounds **L²**, **L⁴**, **7** and **9** for 3 h. After the loading, the cells were washed with PBS and fixed for 20 min at room temperature with PBS + 3% paraformaldehyde. After three washings with PBS, the cells on the coverslips were incubated in 5 μM DRAQ5 for nuclear staining for 20 min at RT, and then washed three times with PBS. After washing, the coverslips were mounted on standard microscope slides with glycerol + 3% *N*-propyl gallate to improve the optical conditions and to prevent photobleaching. The samples were then imaged on a Leica DMRA2 upright microscope by using a 100× 1.4NA objective and a Chroma +A4 UV filter for evaluating anthracene fluorescence ($\lambda_{ex}$ max = 350 nm, $\lambda_{em}$ max = 410 nm) and a Y5 Cy5 red filter for DRAQ5 ($\lambda_{ex}$ max = 647 nm, $\lambda_{em}$ max = 670 nm). Images were acquired and colour-combined by using a CoolSNAP HQ 1.3 Mpixel-cooled CCD camera and the MetaMorph software.

## Acknowledgement

*Margarida Videira, Rute F. Vitor and Isabel Correia wish to thank the Fundação para a Ciência e Tecnologia (National Foundation for Science and Technology) for BI, Doctoral (SFRH/BD/6227/2001) and Postdoctoral (SFRH/BPD/13975/2003) research grants, respectively. The authors would like to acknowledge FEDER and FCT for financial support (POCI/QUI/57632/2004). We wish to acknowledge Dr. Ana Coelho from the Laboratório de Espectrometria de Massa at the Instituto de Tecnologia Química e Biológica, Universidade Nova de Lisboa, Portugal, for the ESI-MS analysis, and Prof. Sílvia Costa from CQE-IST-TU Lisbon for the access to the UV/Vis and fluorescence instrumentation.*

**Keywords:** anthracene derivatives · DNA · pyrazole-containing ligands · radiopharmaceuticals · rhenium

[1] S. Liu, D. S. Edwards, *Bioconjugate Chem.* **2001**, *12*, 7–34.
[2] M. de Jong, W. A. P. Breeman, R. Valkema, B. F. Bernard, E. P. Krenning, *J. Nucl. Med.* **2005**, *46*, 13S–17S.
[3] A. I. Kassis, *J. Nucl. Med.* **2003**, *44*, 1479–1481.
[4] M. Ginj, K. Hinni, S. Tschumi, S. Schulz, H. Maecke, *J. Nucl. Med.* **2005**, *46*, 2097–2103.
[5] P. Häfliger, N. Agorastos, B. Spingler, O. Georgiev, G. Viola, R. Alberto, *ChemBioChem* **2005**, *6*, 414–421.
[6] P. Haefliger, N. Agorastos, A. Renard, G. Giambonini-Brugnoli, C. Marty, R. Alberto, *Bioconjugate Chem.* **2005**, *16*, 582–587.
[7] N. Agorastos, L. Borsig, A. Renard, P. Antoni, G. Viola, B. Spingler, P. Kurz, R. Alberto, *Chem. Eur. J.* **2007**, *13*, 3842–3852.
[8] S. Alves, A. Paulo, J. D. G. Correia, A. Domingos, I. Santos, *J. Chem. Soc. Dalton Trans.* **2002**, 4714–4719.
[9] R. F. Vitor, S. Alves, J. D. G. Correia, A. Paulo, I. Santos, *J. Organomet. Chem.* **2004**, *689*, 4764–4774.
[10] S. Alves, A. Paulo, J. D. G. Correia, L. Gano, C. J. Smith, T. J. Hoffman, Isabel Santos, *Bioconjugate Chem.* **2005**, *16*, 438–449.
[11] S. Alves, J. D. G. Correia, I. Santos, B. Veerendra, G. L. Sieckman, T. J. Hoffman, T. L. Rold, S. D. Figueroa, L. Retzloff, J. McCrate, A. Prasanphanich, C. J. Smith, *Nucl. Med. Biol.* **2006**, *33*, 625–634.
[12] S. Alves, J. D. G. Correia, L. Gano, T. L. Rold, A. Prasanphanich, R. Haubner, M. Rupprich, R. Alberto, C. Decristoforo, I. Santos, C. J. Smith, *Bioconjugate Chem.* **2007**, *18*, 530–537.
[13] W. B. Tan, A. Bhambhani, M. R. Duff, A. Rodger, C. V. Kumar, *Photochem. Photobiol.* **2006**, *82*, 20–30.
[14] R. A. Gardner, J.-G. Delcros, F. Konate, F. Breitbeil III, B. Martin, M. Sigman, M. Huang, Otto Phanstiel IV, *J. Med. Chem.* **2004**, *47*, 6055–6069.
[15] F. Breitbeil III, N. Kaur, J.-G. Delcros, B. Martin, K. A. Abboud, Otto Phanstiel IV, *J. Med. Chem.* **2006**, *49*, 2407–2416.
[16] N. K. Modukuru, K. J. Snow, A. Bhambhani, M. Duff, C. V. Kumar, *J. Phys. Chem. B* **2005**, *109*, 11810–11818.
[17] C. V. Kumar, E. H. A. Punzalan, W. B. Tan, *Tetrahedron* **2000**, *56*, 7027–7040.
[18] N. K. Modukuru, K. J. Snow, B. S. Perrin, Jr., J. Thota, C. V. Kumar, *J. Photochem. Photobiol. A* **2006**, *177*, 43–54.
[19] J. D. McGhee, P. H. von Hippel, *J. Mol. Biol.* **1974**, *86*, 469–486.
[20] H-C. Becker, B. Nordén, *J. Am. Chem. Soc.* **2000**, *122*, 8344–8349.
[21] W. D. Wilson, Y-H. Wang, S. Kusuma, S. Chandrasekaran, N. C. Yang, D. W. Boykin, *J. Am. Chem. Soc.* **1985**, *107*, 4989–4995.
[22] H.-C. Becker, B. Nordén, *J. Am. Chem. Soc.* **1999**, *121*, 11947–11952.
[23] M. R. Duff, W. B. Tan, A. Bhambhani, B. S. Perrin, Jr., J. Thota, A. Rodger, C. V. Kumar, *J. Phys. Chem. B* **2006**, *110*, 20693–20701.
[24] B. Norden, M. Kubista, T. Kurucsev, *Q. Rev. Biophys.* **1992**, *25*, 51–170.
[25] S. James, K. P. Maresca, J. W. Babich, J. F. Valliant, L. Doering, J. Zubieta, *Bioconjugate Chem.* **2006**, *17*, 590–596.
[26] C. A. Vock, W. H. Ang, C. Scolaro, A. D. Phillips, L. Lagopoulos, L. Juillerat-Jeanneret, G. Sava, R. Scopelliti, P. J. Dyson, *J. Med. Chem.* **2007**, *50*, 2166–2175.
[27] M. Bullpitt, W. Kitching, D. Doddrell, W. Adcock, *J. Org. Chem.* **1976**, *41*, 760–766.
[28] J. Ishikawa, H. Sakamoto, S. Nakao, H. Wada, *J. Org. Chem.* **1999**, *41*, 760–766.
[29] R. J. Angelici, *Inorg. Synth.* **1990**, *28*, 162.
[30] R. Alberto, R. Schibli, A. Egli, P. A. Schubiger, W. A. Herrmann, G. Artus, U. Abram, T. A. Kaden, *J. Organomet. Chem.* **1995**, *493*, 119–127.
[31] C. V. Kumar, E. H. Asuncion, *J. Am. Chem. Soc.* **1993**, *115*, 8547–8553.
[32] A. Wada, S. Kozawa, *J. Polym. Sci. Part A* **1964**, *2*, 853–864.

Received: July 30, 2007
Published online on December 5, 2007

  